



HAL
open science

Attitude Estimation and Control Using Linearlike Complementary Filters Theory and Experiment

Lofti Benziane, A. El Hadri, Ali Seba, A. Benallegue, Yacine Chitour

► **To cite this version:**

Lofti Benziane, A. El Hadri, Ali Seba, A. Benallegue, Yacine Chitour. Attitude Estimation and Control Using Linearlike Complementary Filters Theory and Experiment. *IEEE Transactions on Control Systems Technology*, 2016, 24 (6), pp.2133-2140. 10.1109/TCST.2016.2535382 . hal-02307517

HAL Id: hal-02307517

<https://centralesupelec.hal.science/hal-02307517>

Submitted on 3 Apr 2020

HAL is a multi-disciplinary open access archive for the deposit and dissemination of scientific research documents, whether they are published or not. The documents may come from teaching and research institutions in France or abroad, or from public or private research centers.

L'archive ouverte pluridisciplinaire **HAL**, est destinée au dépôt et à la diffusion de documents scientifiques de niveau recherche, publiés ou non, émanant des établissements d'enseignement et de recherche français ou étrangers, des laboratoires publics ou privés.

Attitude Estimation and Control Using Linearlike Complementary Filters: Theory and Experiment

L. Benziane, A. El Hadri, A. Seba, A. Benallegue, and Y. Chitour

Abstract—This brief proposes new algorithms for attitude estimation and control, based on fused inertial vector measurements using a linear complementary filters principle. First, n -order direct and passive complementary filters combined with a TRIaxial Attitude Determination algorithm are proposed to give the attitude estimation solutions. These solutions that are efficient with respect to noise include the gyro-bias estimation. Thereafter, the same principle of data fusion is used to address the problem of attitude tracking based on the inertial vector measurements. Thus, instead of using noisy raw measurements in the control law, a new solution of control that includes a linearlike complementary filter to deal with the noise is proposed. The stability analysis of the tracking error dynamics based on the LaSalle's invariance theorem proved that almost all trajectories converge asymptotically to the desired equilibrium. Simulations and experimental results, obtained with DIY Quad equipped with the APM2.6 autopilot, show the effectiveness and the performance of the proposed solutions.

Index Terms—Attitude Control, attitude estimation, Barbalat's lemma, complementary filters, quadcopter, Lasalle's invariance theorem, Lyapunov analysis.

I. INTRODUCTION

DESPITE the significant existing number of solutions to the attitude estimation and control problems, it remains attractive research topics [1], [2]. The widely used techniques for attitude estimation are based on the extended Kalman filter [1], [3]. Most of these methods are computationally demanding and some of them depending on used attitude representation [4]. Another class of techniques is based on complementary filters [5], [6], which are not so computationally demanding. Due to their simplicity and efficiency, the use of the complementary filters [7, Appendix A] to reconstruct the attitude continues to attract many researchers [7], [8]. In [9], a new strategy by combining a vector-based filter with an optimal attitude determination algorithm has been proposed. The vector-based filter presented in [9] was designed as a

Manuscript received September 7, 2015; revised January 4, 2016; accepted February 20, 2016. Manuscript received in final form February 20, 2016. This work is supported by a public grant overseen by the French National Research Agency (ANR) as part of the Investissement d'Avenir program, through the iCODE Institute project funded by the IDEX Paris-Saclay, ANR-11-IDEX-0003-02. Recommended by Associate Editor Y. Ebihara.

L. Benziane, A. El Hadri, A. Seba, and A. Benallegue are with the Laboratoire d'Ingénierie des Systèmes de Versailles, Université de Versailles Saint Quentin, Versailles 78000, France (e-mail: lotfi.benziane@lsv.uvsq.fr; elhadri@lsv.uvsq.fr; ali.seba@lsv.uvsq.fr; benalleg@lsv.uvsq.fr).

Y. Chitour is with the Laboratoire des signaux et systèmes, Centre National de la Recherche Scientifique, Supélec, Université Paris-Sud XI, Gif-sur-Yvette 91190, France, and also with the Team GECCO, Institut National de Recherche en Informatique et en Automatique, Palaiseau 91120, France (e-mail: yacine.chitour@lss.supelec.fr).

Color versions of one or more of the figures in this paper are available online at <http://ieeexplore.ieee.org>.

Digital Object Identifier 10.1109/TCST.2016.2535382

Kalman filter using linear time variant (LTV) representation of the nonlinear kinematic equation, with observability conclusions given for the LTV reformulation of the original nonlinear system, which can be considered as a theoretical drawback.

Inspired by the approach given in [9], this brief presents globally asymptotically stable filters for the deterministic attitude estimation based on high-order linear complementary filtering. The gyro-bias estimation is also considered. Two forms of filter, termed direct and passive, are designed similarly as the work presented in [7]. The passive form is less sensitive to noise as claimed in [7]. Moreover, the approach proposed here is completely deterministic as it is based on the linear complementary filters followed by the TRIaxial Attitude Determination (TRIAD) algorithm [10, Sec. II-C] for the attitude estimation. As a matter of fact, the TRIAD is the deterministic attitude estimation algorithm par excellence as claimed by [11]. Although it was proved that the TRIAD is less accurate than other optimal approaches [11], it will be shown throughout this brief that it is possible to obtain higher quality of the attitude estimation when this approach is used.

Most of the traditional rigid body attitude control approaches given in the literature are based on the feedback scheme using the attitude estimation [12]–[14]. In fact, the explicit use of the attitude in the control law involves the determination of attitude from measurements. An excellent review of the basic control design and feedback control for underactuated vertical takeoff and landing (VTOL) aircraft type can be found in [15]. A quaternion-based feedback was used in [13], [16], and [17] to stabilize the attitude of a VTOL. Recently, some authors have proposed to use directly the raw vector measurements to perform the attitude stabilization [18]–[20]. Frequently, the implementations of some attitude controllers using directly the raw vector measurements are confronted with noises. Therefore, a novel filter to improve the performance of the attitude tracking controller is proposed. The attitude controller is based on the filtered vector measurements while ensuring an almost global asymptotic stability without using the attitude measurements. Although unit quaternions are used in a stability analysis, the unwinding phenomenon is avoided.

The result presented in this brief extends those from [10]. The first contribution of this brief is the extension of the global convergence of the direct and passive complementary filters to the case of n -order, which gives the advantage to improve the quality of estimation by choosing the adequate order and form of the filter. Another contribution is the design of a new control law based on filtered inertial vectors and rate-gyro measurements to control the attitude of a rigid

body without using the attitude measurements, for which an almost global stability is given. All our contributions are validated by simulations and experiments on the DIY drone Quadcopter [21].

II. PRELIMINARIES

A. Mathematical Background and Notations

Attitude of the rigid body represents the relative orientation of $\{\mathcal{B}\}$ with respect to $\{\mathcal{I}\}$, where $\{\mathcal{B}\}$ denotes the mobile body-frame fixed to its center of mass and $\{\mathcal{I}\}$ denotes the inertial reference frame attached to the 3-D space. In this brief, the attitude of the rigid body will be described using either rotation matrices $R \in \text{SO}(3)$ or quaternions $\begin{bmatrix} q_0 \\ \mathbf{q} \end{bmatrix} \in \mathbb{S}^3$ [22], where $\text{SO}(3)$ is the special orthogonal group, \mathbb{S}^3 is the unit sphere, and \odot denotes the quaternions multiplication on \mathbb{S}^3 , as defined in [7, Appendix B]. Denote by $S(\cdot)$ the skew-symmetric matrix defined such that for any $x, y \in \mathbb{R}^3$, $S(x)y = x \times y$, where \times denotes the vector cross product and

$$S(x) = \begin{bmatrix} 0 & -x_3 & x_2 \\ x_3 & 0 & -x_1 \\ -x_2 & x_1 & 0 \end{bmatrix}, \quad x = \begin{bmatrix} x_1 \\ x_2 \\ x_3 \end{bmatrix}. \quad (1)$$

The mapping $\mathcal{R} : \mathbb{S}^3 \rightarrow \text{SO}(3)$ is defined by the Euler–Rodriguez formula as follows:

$$\mathcal{R}(q_0, \mathbf{q}) = I_d + 2q_0S(\mathbf{q}) + 2S(\mathbf{q})^2 \quad (2)$$

where I_d is the 3×3 identity matrix.

For any two vectors $x, y \in \mathbb{R}^3$ and rotation matrix $R \in \text{SO}(3)$, the following identities hold: $S(x)y = -S(y)x$, $S(S(x)y) = S(x)S(y) - S(y)S(x)$, $S(x)^2 = xx^T - x^T x I_d$, and $S(Rx) = RS(x)R^T$.

If n is a positive integer, set $e_n = (0, \dots, 0, 1)^T$. To every $\gamma = (\gamma_1, \dots, \gamma_n) \in \mathbb{R}^n$, we associate the polynomial

$$P_\gamma(s) = s^n + \sum_{k=1}^n \gamma_k s^{n-k} \quad (3)$$

and the companion matrix A_γ

$$A_\gamma = \begin{pmatrix} 0 & 1 & 0 & \cdots & 0 \\ 0 & 0 & 1 & \ddots & \vdots \\ \vdots & \vdots & \ddots & \ddots & 0 \\ 0 & 0 & \cdots & 0 & 1 \\ -\gamma_n & -\gamma_{n-1} & \cdots & -\gamma_2 & -\gamma_1 \end{pmatrix} \quad (4)$$

whose characteristic polynomial is P_γ . Use $\pi : \mathbb{R}^n \rightarrow \mathbb{R}^{n-1}$ to denote the projection onto \mathbb{R}^{n-1} , i.e., $\pi(\gamma) = (\gamma_1, \dots, \gamma_{n-1})$. Define the following subsets of \mathbb{R}^n , $\mathcal{H}_n = \{\gamma \in \mathbb{R}^n \mid P_\gamma \text{ Hurwitz}\}$ and $\overline{\mathcal{H}}_n = \{\gamma \in \mathcal{H}_n \mid \pi(\gamma) \in \mathcal{H}_{n-1}\}$.

The proof of the following lemma is deferred in the Appendix.

Lemma 1: If n is a positive integer, then $\overline{\mathcal{H}}_n$ is not empty.

Note 1: Let $E \in \mathbb{R}^{(n \times n)}$ and $\sigma(E) = \{\lambda_1, \dots, \lambda_n\}$ its spectrum, where $\lambda_l, l = 1 \dots n$ are the eigenvalues of E . Let $I_k \in \mathbb{R}^{(k \times k)}$, k integer, be the identity matrix. Then, the spectrum of the Kronecker product of E by I_k , $E \otimes I_k \in \mathbb{R}^{(kn \times kn)}$, is equal to $\sigma(E)$ according to [23, Th., p. 245]. In particular, $E \otimes I_k$ is Hurwitz if and only if E is.

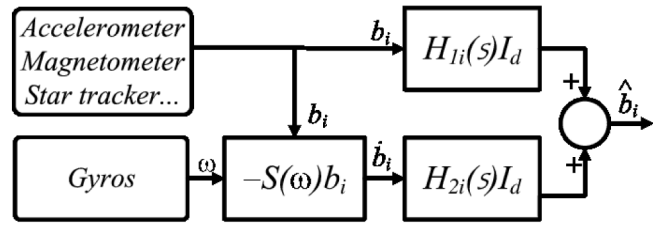


Fig. 1. Classical form of complementary filters.

The rigid body rotational motion can be described by its kinematic and dynamic equations

$$\begin{bmatrix} \dot{q}_0(t) \\ \dot{\mathbf{q}}(t) \end{bmatrix} = \begin{bmatrix} -\frac{1}{2}q^T(t)\omega(t) \\ \frac{1}{2}(q_0(t)I_d + S(\mathbf{q}(t)))\omega(t) \end{bmatrix} \quad (5)$$

$$J\dot{\omega}(t) = -S(\omega(t))J\omega(t) + \tau(t) \quad (6)$$

where $\omega(t)$ is the angular velocity of the rigid body and $\tau(t)$ is the applied torque to the system, both expressed in $\{\mathcal{B}\}$. $J \in \mathbb{R}^{3 \times 3}$ is a symmetric positive definite constant inertia matrix about the center of mass of the rigid body.

Now, given a constant vector r in $\{\mathcal{I}\}$, then its corresponding vector in $\{\mathcal{B}\}$ is given by $b(t) = R^T(t)r$ and

$$\dot{b}(t) = -S(\omega(t))b(t). \quad (7)$$

Consider the following rate-gyros model:

$$\omega_m(t) = \omega(t) + \eta \quad (8)$$

where $\omega_m(t)$ is the measured angular velocity and η is the real unknown gyro bias.

In all what follows, the indices $i = 1, \dots, m$ denote the number of the used inertial vectors.

B. Sensor-Based Attitude Estimation Approach Using Complementary Filters

The sensor-based attitude estimation approach, mentioned in [9], is consisting of two steps process: first, filter sensor measurements, and then determine attitude. Inspired by this approach, a new structure of the complementary filters is proposed. Indeed, the complementary filters give us a mean to fuse multiple heterogeneous independent noisy measurements of the same signal that have complementary spectral characteristics [7]. The classical form of the complementary filters is shown in Fig. 1. In this case, the complementarity filtering is achieved if the following condition is satisfied:

$$H_{1i}(s) + sH_{2i}(s) = 1, \quad i = 1, \dots, m \quad (9)$$

where s is the Laplace variable, $H_{1i}(s)$ is a low-pass filter, and $sH_{2i}(s)$ is a high-pass filter.

From the structure of the classical form of a complementary filter, the estimate \hat{b}_i of the state b_i by fusing measurements of the i th inertial direction vectors and gyro measurements can be written as

$$\hat{b}_i = H_{1i}(s)b_i + H_{2i}(s)\dot{b}_i, \quad i = 1, \dots, m. \quad (10)$$

Now, for the determination of the attitude, the complementary filter can be followed by any algebraic algorithm like

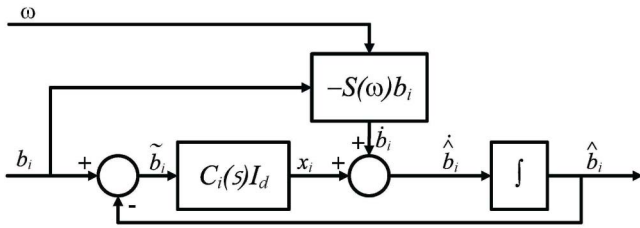


Fig. 2. Direct linearlike complementary filter.

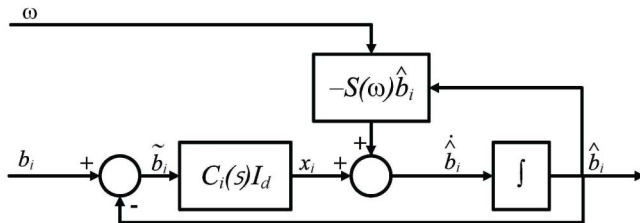


Fig. 3. Passive linearlike complementary filter.

the TRIAD algorithm. Despite the fact that the TRIAD is known less accurate than other statistical algorithms based on minimizing Wahba's loss function [11], we will show that we can obtain good results by using fused data. The choice of the TRIAD algorithm is justified by the fact that the optimal algorithms are usually much slower than the deterministic algorithms [11].

The first problem addressed in this brief is the design of an attitude and heading reference system using the concept of the sensor-based attitude estimation approach [9]. The goal is to prove that it is possible to obtain a structure based on a deterministic complementary linear filter with a globally asymptotic convergence. The filtered data will be used by a TRIAD for the attitude determination as explained before. The second problem addressed is to prove that the use of estimated measurements by the complementary filters can achieve attitude tracking with an almost global stability.

Along this brief, the following assumptions will be used.

Assumption 1: Assume the existence of m measured vectors $b_i(t)$, $i = 1, \dots, m$ expressed in $\{\mathcal{B}\}$, and then, at least two of them are noncollinear.

Assumption 2: Assume that the real unknown gyro bias η is bounded and constant (or slowly varying), such that $\dot{\eta} = 0$. Moreover, assume that the measured angular velocities $\omega_m(\cdot)$ are bounded as well.

III. DESIGN OF THE LINEARLIKE COMPLEMENTARY FILTERS

The classical form of the complementary filters can be reformulated in the feedback form, as shown in Fig. 2. Two structures of the complementary filter are proposed. The first one termed direct linearlike complementary filter and the second one termed passive linearlike complementary filter. In the first one, the offsetting of nonlinear term uses direct raw measurements, as shown in Fig. 2, while in the second one, the filtered measurements are used, as shown in Fig. 3.

From the equivalence between the classical form and the feedback form, one can get $H_{1i}(s) = (C_i(s)/s + C_i(s))$ and $H_{2i}(s) = (1/s + C_i(s))$, where $C_i(s)$ represents the compensator term in the feedback form. One can write the compensator term as

$$C_i(s) = \frac{sH_{1i}(s)}{1 - H_{1i}(s)}, \quad i = 1, \dots, m. \quad (11)$$

The design of the compensator $C_i(s)$ can be achieved by choosing the adequate filter order for improving the quality of estimation. Consider now, for $i = 1, \dots, m$, the general n -order transfer function $H_{1i}(s)$ by first taking $\mathcal{Y}_i = (\gamma_{i1}, \dots, \gamma_{in}) \in \mathcal{H}_n$ and setting $H_{1i}(s) = (\gamma_{in}/P_{\mathcal{Y}_i}(s))$, where $P_{\mathcal{Y}_i}(s)$ and γ_{in} are defined by (3). Using (11), one can obtain

$$C_i(s) = \frac{\gamma_{in}}{P_{\pi(\mathcal{Y}_i)}(s)}, \quad i = 1, \dots, m. \quad (12)$$

A. High-Order Direct Linearlike Complementary Filters

Consider system (14) and the block diagram of the direct form in Fig. 2 with compensator $C_i(s)$ given by (12) for $i = 1, \dots, m$. Then, the closed-loop dynamics with gyro-bias estimation for any n -order is given for $i = 1, \dots, m$ by

$$\begin{cases} \dot{x}_i^{(n-1)} = -\sum_{k=1}^{n-1} \gamma_{ik} x_i^{(n-k-1)} + \gamma_{in}(b_i - \hat{b}_i) \\ \dot{\hat{b}}_i = -S(\omega_m - \hat{\eta})b_i + x_i \\ \dot{\hat{\eta}} = \Gamma_d \sum_{i=1}^m S(b_i)v_i \end{cases} \quad (13)$$

where $x_i^{(j)}$ is the j th derivative of x_i with $x_i^{(0)} = x_i$, γ_{ik} , $i = 1, \dots, m$, $k = 1, \dots, n$ are the components of $\mathcal{Y}_i = (\gamma_{i1}, \dots, \gamma_{in}) \in \mathcal{H}_n$, Γ_d is a real positive definite diagonal matrix gain, and v_i is a vector to be defined later.

First, using (7) and (8), one can write the following system:

$$\begin{cases} \dot{b}_i = -S(\omega_m - \eta)b_i \\ \dot{\eta} = 0. \end{cases} \quad (14)$$

Define the observation errors

$$\tilde{b}_i = b_i - \hat{b}_i, \quad i = 1, \dots, m \quad (15)$$

$$\tilde{\eta} = \eta - \hat{\eta} \quad (16)$$

then using (7) and (13)–(16), yield the following error dynamics:

$$\begin{cases} \dot{x}_i^{(n-1)} = -\sum_{k=1}^{n-1} \gamma_{ik} x_i^{(n-k-1)} + \gamma_{in} \tilde{b}_i \\ \dot{\tilde{b}}_i = -S(b_i) \tilde{\eta} - x_i \\ \dot{\tilde{\eta}} = -\Gamma_d \sum_{i=1}^m S(b_i)v_i. \end{cases} \quad (17)$$

By the evaluation of the time derivative of the first equation of (17), one can rewrite (17) as

$$\begin{cases} \dot{x}_i^{(n)} = -\sum_{k=1}^n \gamma_{ik} x_i^{(n-k)} - \gamma_{in} S(b_i) \tilde{\eta} \\ \dot{\tilde{\eta}} = -\Gamma_d \sum_{i=1}^m S(b_i)v_i. \end{cases} \quad (18)$$

Now, consider the new state vector $z_i \in \mathbb{R}^{3n}$, $i = 1, \dots, m$, such as $z_i^T = [x_i^T, \dot{x}_i^T, \dots, x_i^{(n-1)T}]$, and define the vectors v_i to be

$$v_i = B_{di}^T P_{di} z_i, \quad i = 1, \dots, m. \quad (19)$$

One can rewrite (18) as

$$\begin{cases} \dot{z}_i(t) = A_{di}z_i(t) + B_{di}S(\tilde{\eta})b_i \\ \dot{\tilde{\eta}} = -\Gamma_d \sum_{i=1}^m S(b_i)B_{di}^T P_{di}z_i \end{cases} \quad (20)$$

where $i = 1, \dots, m$ and the Hurwitz matrices $A_{di} = A\gamma_i \otimes I_d \in \mathbb{R}^{(3n \times 3n)}$ [$A\gamma_i$ is defined by (4)], $B_{di} = \gamma_{in}e_n \otimes I_3 \in \mathbb{R}^{3n \times 3}$, and the matrices $P_{di} \in \mathbb{R}^{(3n \times 3n)}$ are real symmetric positive definite solutions of the following Lyapunov equations for given symmetric positive definite matrices Q_{di} :

$$A_{di}^T P_{di} + P_{di} A_{di} = -Q_{di}, \quad i = 1, \dots, m. \quad (21)$$

Now, the first result can be stated.

Proposition 1: Consider the filter (13) with (19), under Assumptions 1 and 2, then the errors (15) and (16) converge globally asymptotically to zero.

Proof: Consider the following Lyapunov function candidate:

$$V_1 = \sum_{i=1}^m z_i^T P_{di} z_i + \tilde{\eta}^T \Gamma_d^{-1} \tilde{\eta} \quad (22)$$

where $P_{di} \in \mathbb{R}^{(3n \times 3n)}$, $i = 1, \dots, m$ is given by (21). Using (21) and the fact that $\tilde{\eta}^T S(b_i)B_{di}^T P_{di} z_i = z_i^T P_{di} B_{di} S(\tilde{\eta})b_i$, the time derivative of (22) in view of (20) is given by $\dot{V}_1 = -\sum_{i=1}^m z_i^T Q_{di} z_i \leq 0$. Therefore, z_i and $\tilde{\eta}_i$ are bounded, and consequently, by using (20), \dot{z}_i and $\dot{\tilde{\eta}}_i$ are bounded. The evaluation of the second derivative of (22) in view of (20) gives $\ddot{V}_1 = -\sum_{i=1}^m z_i^T G z_i + 2z_i^T Q_{di} B_{di} S(b_i) \tilde{\eta}$ with $G = A_{di}^T Q_{di} + Q_{di} A_{di}$, \ddot{V}_1 is clearly bounded. By Barbalat's lemma, $\lim_{t \rightarrow \infty} \dot{V}_1(t) = 0$ and consequently $\lim_{t \rightarrow \infty} z_i(t) = 0$. Then, according to (17), one can obtain $\lim_{t \rightarrow \infty} \hat{b}_i(t) = 0$. Next, one can evaluate the second time derivative of z_i and conclude that all terms are bounded. Thus, using Barbalat's lemma, $\lim_{t \rightarrow \infty} \dot{z}_i(t) = 0$. Therefore, using (20) and $\lim_{t \rightarrow \infty} z_i(t) = 0$, one can conclude that $B_{di} S(b_i) \tilde{\eta}$ converges to zero and equivalently $\lim_{t \rightarrow \infty} S(b_i(t)) \tilde{\eta}(t) = 0$. Under Assumption 1, one can conclude that $\lim_{t \rightarrow \infty} \tilde{\eta}(t) = 0$. \square

Remark 1: One can obtain the first-order direct filter as

$$\begin{cases} \dot{\hat{b}}_i = -S(\omega_m - \hat{\eta})b_i + \gamma_{i1}(b_i - \hat{b}_i) \\ \dot{\hat{\eta}} = \Gamma_1 \sum_{i=1}^m S(b_i) \hat{b}_i. \end{cases} \quad (23)$$

B. High-Order Passive Linearlike Complementary Filters

In the passive form, the design of the complementary filter is performed by injecting filtered measurements for the offsetting nonlinear term, as shown in block diagram of Fig. 3, with a compensator $C_i(s)$, $i = 1, \dots, m$, defined by (12). Then, the following new n -order passive form with the gyro-bias estimation is proposed:

$$\begin{cases} \dot{x}_i^{(n-1)} = -\sum_{k=1}^{n-1} \gamma_{ik} x_i^{(n-k-1)} + \gamma_{in}(b_i - \hat{b}_i) \\ \dot{\hat{b}}_i = -S(\omega_m - \hat{\eta}) \hat{b}_i + w_i \\ \dot{\hat{\eta}} = -\Gamma_p \sum_{i=1}^m S(b_i) \hat{b}_i \end{cases} \quad (24)$$

where $i = 1, \dots, m$, $x_i^{(j)}$ is the j th order derivative of x_i with $x_i^{(0)} = x_i$, γ_{ik} , $i = 1, \dots, m$, $k = 1, \dots, (n-1)$ are

components of $\pi(\gamma_i) = (\gamma_{i1}, \dots, \gamma_{i(n-1)})$ for $\gamma_i \in \overline{\mathcal{H}}_n$, Γ_p is a real positive definite diagonal matrix gain, and w_i is given by

$$w_i = B_{pi}^T P_{pi} X_i \quad (25)$$

with $X_i \in \mathbb{R}^{3(n-1)}$, $i = 1, \dots, m$, such as $X_i^T = [x^T, \dot{x}^T, \dots, x^{(n-2)T}]$, allowing to rewrite (24) as

$$\begin{cases} \dot{X}_i(t) = A_{pi} X_i(t) + B_{pi}(b_i - \hat{b}_i) \\ \dot{\hat{b}}_i = -S(\omega_m - \hat{\eta}) \hat{b}_i + B_{pi}^T P_{pi} X_i \\ \dot{\hat{\eta}} = -\Gamma_p \sum_{i=1}^m S(b_i) \hat{b}_i \end{cases} \quad (26)$$

where the Hurwitz matrices $A_{pi} = A\pi(\gamma_i) \otimes I_d \in \mathbb{R}^{(3(n-1) \times 3(n-1))}$ [$A\pi(\gamma_i)$ is defined by (4), see Note 1 for A_{pi} Hurwitz] and the matrices $B_{pi} = \gamma_{in}e_{(n-1)} \otimes I_d \in \mathbb{R}^{3(n-1) \times 3}$. The matrices $P_{pi} \in \mathbb{R}^{(3(n-1) \times 3(n-1))}$, $i = 1, \dots, m$, are real symmetric positive definite solutions of the following Lyapunov equations for given symmetric positive definite matrices Q_{pi} :

$$A_{pi}^T P_{pi} + P_{pi} A_{pi} = -Q_{pi}. \quad (27)$$

Now, the second result can be stated.

Proposition 2: Consider the filter (24) with (25), under Assumptions 1 and 2, then the errors (15) and (16) converge globally asymptotically to zero.

Proof: First, let us evaluate the error dynamics of (26). Using (7), (15), and (16), one can obtain

$$\begin{cases} \dot{X}_i(t) = A_{pi} X_i(t) + B_{pi} \tilde{b}_i \\ \dot{\tilde{b}}_i = -S(b_i) \tilde{\eta} + S(\tilde{b}_i)(\omega + \tilde{\eta}) - B_{pi}^T P_{pi} X_i \\ \dot{\tilde{\eta}} = -\Gamma_p \sum_{i=1}^m S(b_i) \tilde{b}_i. \end{cases} \quad (28)$$

Consider now, the following Lyapunov function:

$$V_2 = \sum_{i=1}^m X_i^T P_{pi} X_i + \sum_{i=1}^m \tilde{b}_i^T \tilde{b}_i + \tilde{\eta}^T \Gamma_p^{-1} \tilde{\eta} \quad (29)$$

using (27), the time derivative of (29) in view of (28) is given by $\dot{V}_2 = -\sum_{i=1}^m X_i^T Q_{pi} X_i \leq 0$. Therefore, X_i , \tilde{b}_i , and $\tilde{\eta}_i$ are bounded, and consequently, from (28) and Assumption 2, \dot{X}_i , $\dot{\tilde{b}}_i$, and $\dot{\tilde{\eta}}_i$ are also bounded. The rest of the proof is similar to the proof of Proposition 1. It is easy to verify that \dot{V}_2 is bounded. Thus, using Barbalat's lemma, $\lim_{t \rightarrow \infty} \dot{V}_2(t) = 0$, and consequently, $\lim_{t \rightarrow \infty} X_i(t) = 0$. In addition, \dot{X}_i is bounded, then $\lim_{t \rightarrow \infty} \dot{X}_i(t) = 0$, and using (28), $\lim_{t \rightarrow \infty} \tilde{b}_i(t) = 0$. By a standard reasoning by contradiction, one gets that $\lim_{t \rightarrow \infty} \tilde{b}_i(t) = 0$. Using this fact and (28), therefore $\lim_{t \rightarrow \infty} S(b_i) \tilde{\eta} = 0$. Under Assumption 1, one can conclude that $\lim_{t \rightarrow \infty} \tilde{\eta}(t) = 0$. \square

Remark 2: One can obtain the first-order passive filter as

$$\begin{cases} \dot{\hat{b}}_i = -S(\omega_m - \hat{\eta}) \hat{b}_i + \gamma_{i1}(b_i - \hat{b}_i) \\ \dot{\hat{\eta}} = \Gamma_2 \sum_{i=1}^m S(b_i) \hat{b}_i. \end{cases} \quad (30)$$

IV. SENSOR-BASED ATTITUDE TRACKING

As a logical sequel to the proposed solutions to the problem of attitude estimation, a new sensor-based attitude control law that uses only filtered inertial vectors and rate-gyro measurements to track the desired attitude without using attitude measurements is proposed. In this section, it is assumed that $\omega_m(t) = \omega(t)$.

A. Controller Design

First, let us define the orientation error by $\bar{R}(t) = R(t)R_d^T(t)$, which corresponds to the quaternion error $\begin{bmatrix} \bar{q}_0(t) \\ \bar{q}(t) \end{bmatrix} \in \mathbb{S}^3$ whose dynamics is governed by

$$\begin{bmatrix} \dot{\bar{q}}_0 \\ \dot{\bar{q}} \end{bmatrix} = \begin{bmatrix} -\frac{1}{2}\bar{q}^T R_d \tilde{\omega} \\ \frac{1}{2}(\bar{q}_0 I_d + S(\bar{q}))R_d \tilde{\omega} \end{bmatrix} \quad (31)$$

where time indices are omitted, $\tilde{\omega} = \omega - \omega_d$, ω is the time-varying angular velocity of the rigid body expressed in $\{\mathcal{B}\}$, ω_d is the time-varying desired angular velocity, and R_d is the time-varying desired rotation matrix. Now, the following new filter for the control problem with the new control law is proposed as:

$$\dot{\hat{b}}_i = \alpha_i \tilde{b}_i + S(\omega_d) \tilde{b}_i - S(\omega) b_i + \delta_i S(b_i^d) \tilde{\omega} \quad (32)$$

$$\begin{aligned} \tau = & (S(\omega)J - JS(\omega_d))\omega + J \sum_{i=1}^m \rho_i S(b_i^d) \hat{b}_i \\ & + J\dot{\omega}_d - kJ\tilde{\omega} \end{aligned} \quad (33)$$

where time indices are omitted, $\alpha_i > 0$, $\delta_i > 0$, $\rho_i > 0$, b_i , $i = 1, \dots, m$ are the inertial measurements, and $\tilde{b}_i = b_i - \hat{b}_i$. Define the following tracking errors $\tilde{\omega} = R_d(\omega - \omega_d)$ and $\tilde{b}_i = R_d(b_i - \hat{b}_i)$. Then, one can obtain the following error dynamics:

$$\dot{\tilde{\omega}} = R_d S(\omega_d) \omega + R_d (\dot{\omega} - \dot{\omega}_d) \quad (34)$$

$$\dot{\tilde{b}}_i = -\alpha_i \tilde{b}_i - \delta_i S(r_i) \tilde{\omega}. \quad (35)$$

Then, the torque $\tau(t)$ can be rewritten as

$$\begin{aligned} \tau = & S(\omega)J\omega - JS(\omega_d)\omega + J\dot{\omega}_d - kJR_d^T \tilde{\omega} \\ & - 2JR_d^T(\bar{q}_0 I_d - S(\bar{q}))W\bar{q} - JR_d^T \sum_{i=1}^m \rho_i S(r_i) \tilde{b}_i \end{aligned} \quad (36)$$

where [20, Lemma 1] is used to rewrite the term $\sum_{i=1}^m \rho_i S(b_i^d) b_i$, $W = -\sum_{i=1}^m \rho_i S(r_i)^2$, and W is a positive definite matrix [20, Lemma 2] and supposed to have simple eigenvalues (see [18, Lemma 1] to justify this hypothesis). Finally, using (6), (31), and (34)–(36), one can obtain the following closed-loop dynamics:

$$\begin{cases} \dot{\tilde{b}}_i(t) = -\alpha_i \tilde{b}_i(t) - \delta_i S(r_i(t)) \tilde{\omega}(t) \\ \dot{\bar{q}}_0(t) = -\frac{1}{2} \bar{q}^T(t) \tilde{\omega}(t) \\ \dot{\bar{q}}(t) = \frac{1}{2} (\bar{q}_0(t) I_d + S(\bar{q}(t))) \tilde{\omega}(t) \\ \dot{\tilde{\omega}}(t) = -2(\bar{q}_0(t) I_d - S(\bar{q}(t))) W \bar{q}(t) \\ \quad - \sum_{i=1}^m \rho_i S(r_i) \tilde{b}_i(t) - k \tilde{\omega}(t). \end{cases} \quad (37)$$

Denote by $\mathbf{0}_{3m}$ the $3 \times m$ zero matrix and define the state $\Theta := (\bar{b}_1, \dots, \bar{b}_m, \bar{Q}, \tilde{\omega})$. The closed-loop dynamics (37) can be rewritten as $\dot{\Theta} = G(\Theta)$, such that $\Theta \in \Delta$ and $\Delta := \mathbb{R}^{3m} \times \mathbb{S}^3 \times \mathbb{R}^3$, and define the following positive radially unbounded function: $V_3 : \Delta \rightarrow \mathbb{R}$:

$$V_3(\Theta) = \sum_{i=1}^m \frac{\rho_i}{\delta_i} \bar{b}_i^T \bar{b}_i + 4\bar{q}^T W \bar{q} + \tilde{\omega}^T \tilde{\omega}. \quad (38)$$

Theorem 1: Consider system (5) and (6) and the control law (33) with the observer given by (32). Under Assumption 1, the following holds.

- 1) The equilibria of the closed-loop system (37) are defined by $\Theta_1^\pm = (\mathbf{0}_{3m}, [\pm 1], \mathbf{0})$ and $\Theta_{2,3,4}^\pm = (\mathbf{0}_{3m}, [\pm v_j], \mathbf{0})$, where v_j , $j = 1, 2, 3$ are the eigenvectors of W .
- 2) The equilibria Θ_1^\pm are asymptotically stable with a domain of attraction containing the set $C_a^+ := \{\Theta \in \Delta \mid V_3(\Theta) < 4\lambda_{\min}(W) \text{ and } \bar{q}_0 > 0\}$, for Θ_1^+ and $C_a^- := \{\Theta \in \Delta \mid V_3(\Theta) < 4\lambda_{\min}(W) \text{ and } \bar{q}_0 < 0\}$, for Θ_1^- , where $\lambda_{\min}(W)$ is the smallest eigenvalue of W .
- 3) The equilibria $\Theta_{2,3,4}^\pm$ are locally unstable and Θ_1^\pm are almost globally asymptotically stable.

Proof: The proof of the first item is similar to the proof of [18, Th. 1]. Recall that the closed-loop dynamics (37) is autonomous, therefore it is possible to use LaSalle's invariance theorem to prove the second item. Note that the time derivative of (38) using (37) is given by $\dot{V}_3(\Theta) = -2k\tilde{\omega}(t)^T \tilde{\omega}(t) - 2 \sum_{i=1}^m \alpha_i (\rho_i / \delta_i) \tilde{b}_i(t)^T \tilde{b}_i(t) \leq 0$ and the proof of item 2) will be similar to the proof of [18, Th. 1].

Let us prove that the equilibria $\Theta_{2,3,4}^\pm$ are unstable. Since the only difference between these equilibria is the value of the eigenvector, the proof is given only for $\Theta_2^+ \in \Delta$. The other cases will be similar. To do this, we consider $\Theta_2^* := (\bar{b}_1^*, \dots, \bar{b}_m^*, \bar{Q}^*, \tilde{\omega}^*)$ a neighborhood of Θ_2^+ (arbitrary close), and since the function V_3 is nonincreasing, it suffices to prove that $V_3(\Theta_2^*) - V_3(\Theta_2^+) < 0$. Let us use the following change of variable:

$$\begin{bmatrix} \bar{q}_0^* \\ \bar{q}^* \end{bmatrix} = \begin{bmatrix} 0 \\ v_1 \end{bmatrix} \odot \begin{bmatrix} x_0 \\ x \end{bmatrix} = \begin{bmatrix} -v_1^T x \\ x_0 v_1 + S(v_1) x \end{bmatrix}. \quad (39)$$

Using (39) and the fact that $Wv_1 = \lambda_1 v_1$ (where λ_1 is the eigenvalue associated with the unit eigenvector v_1 of W), one can evaluate $D = V_3(\Theta_2^*) - V_3(\Theta_2^+)$ as follows: $D = \sum_{i=1}^m (\rho_i / \delta_i) \bar{b}_i^{*T} \bar{b}_i^* + \tilde{\omega}^{*T} \tilde{\omega}^* + 4\lambda(x_0^2 - 1) - 4x^T S(v_1) W S(v_1) x$. If we take x close to v_2 such that $x = \varepsilon v_2$, where $\varepsilon > 0$ sufficiently small, the unit quaternion constraint gives $x_0^2 = 1 - \varepsilon^2$. In this case, one can get $D = \sum_{i=1}^m (\rho_i / \delta_i) \bar{b}_i^{*T} \bar{b}_i^* + \tilde{\omega}^{*T} \tilde{\omega}^* - 4\lambda_1 \varepsilon^2$ which means that if $\varepsilon^2 > (1/4\lambda_1) (\sum_{i=1}^m (\rho_i / \delta_i) \bar{b}_i^{*T} \bar{b}_i^* + \tilde{\omega}^{*T} \tilde{\omega}^*)$ then $D < 0$. As a result, there exists Θ_2^* arbitrary close to Θ_2^+ , such that $V_3(\Theta_2^*) < V_3(\Theta_2^+)$, and since the function V_3 is nonincreasing, it is clear that Θ_2^+ is unstable. Similarly, all equilibria $\Theta_{2,3,4}^\pm$ are unstable. Finally, in the state space Δ , the set of unstable equilibria is Lebesgue measure zero. Therefore, almost all trajectories converge asymptotically to Θ_1^\pm . \square

TABLE I
STANDARD DEVIATION OF EULER ANGLES ERRORS

| | Direct form | | | Passive form | | |
|-----------|----------------------------|---------------------------|-------------------------|----------------------------|---------------------------|-------------------------|
| | $\sigma_\varphi(^{\circ})$ | $\sigma_\theta(^{\circ})$ | $\sigma_\psi(^{\circ})$ | $\sigma_\varphi(^{\circ})$ | $\sigma_\theta(^{\circ})$ | $\sigma_\psi(^{\circ})$ |
| 1st order | 1.2162 | 0.9597 | 1.8076 | 1.2089 | 0.9570 | 1.7937 |
| 2nd order | 0.9028 | 0.6727 | 1.3118 | 0.8830 | 0.6557 | 1.2782 |
| 3rd order | 0.8216 | 0.6122 | 1.2100 | 0.8023 | 0.5908 | 1.1829 |

Remark 3: In the case of stabilization ($\omega_d = 0$), the control law (33) with the filter (32) can be modified to get

$$\hat{b}_{si} = \alpha_i(b_i - \hat{b}_{si}) - S(\omega)b_i + \delta_i S(b_i^d)\omega \quad (40)$$

$$\tau_s = \sum_{i=1}^m \rho_i S(b_i^d) \hat{b}_{si} - k\omega. \quad (41)$$

V. SIMULATIONS AND EXPERIMENTAL RESULTS

In this section, we present some simulation and experimental results showing the effectiveness and the performances of the proposed solutions. The considered observed vectors are $b_1 = a = [a_x \ a_y \ a_z]^T$ (m/s²) for accelerometer measurements and $b_2 = m = [m_x \ m_y \ m_z]^T$ (normalized) for magnetometer measurements expressed in north-east-down reference frame. The corresponding fixed gravitational earth vector and the magnetic earth field vector are $r_1 = [0, 0, 1]^T$ and $r_2 = [0.434, -0.04, 0.899]^T$, respectively, both normalized.

A. Importance of Filter Order and Form for Attitude Estimation

To show the effectiveness and performances of the proposed filters for attitude estimation, many simulations were done. Three cases were selected, depending on the order of the filters. The selected transfer functions are $H_{1i}(s) = (\gamma_{in}/P\gamma_i(s)) = (\alpha^n/(s + \alpha)^n)$, for $i = 1, 2$ and $n = 1, 2, 3$. α was set to 10 for all cases, $\Gamma_d = \Gamma_p = 0.1I_d$. For the direct second-order and passive third-order $Q_{di} = Q_{pi} = I_{6 \times 6}$, $i = 1, 2$, and for the direct third-order, $Q_{di} = I_{9 \times 9}$, $i = 1, 2$. An additive centered zero-mean white noise was taken for measurements with standard deviation 0.1(normalized) for accelerometer and magnetometer, 1 ($^{\circ}$ /s) for rate gyros. The measurements from gyroscope $\omega_m(t)$ (rad/s) are also corrupted by a constant bias $\eta = [2, -3, 1]$ ($^{\circ}$ /s). The standard deviations $\sigma_\varphi, \sigma_\theta, \sigma_\psi$ of Euler angles errors are shown in Table I. It is clear that choosing a high order improves the quality of estimation. In addition, as claimed, the passive form is less sensitive to noise compared with the direct one.

B. Importance of Filtered Observed Vectors for Attitude Control

The advantage of the novel sensor-based control law (33) presented in this brief is the use of the data fusion to improve the attitude tracking. To show the impact of using the filtered measurements \hat{b}_i , one can generate a raw control torque by replacing \hat{b}_i in (33) with the raw measurements b_i , which can be denoted by τ_n . Simulations have been

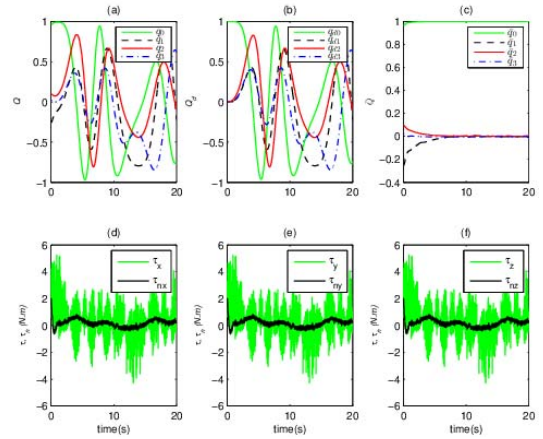


Fig. 4. Attitude tracking simulation results: (a) Real quaternion trajectories. (b) Desired quaternion trajectories. (c) Quaternion errors. (d) τ_x compared to τ_{nx} . (e) τ_y compared to τ_{ny} . (f) τ_z compared to τ_{nz} .

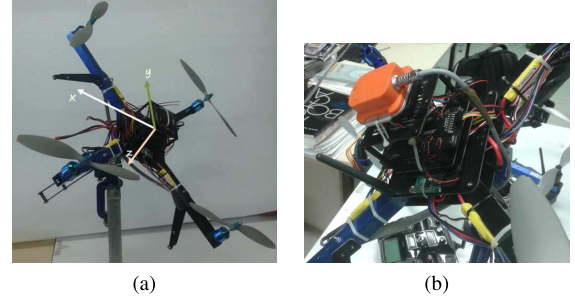


Fig. 5. Test-bench DIY Quad. (a) Test-bench. (b) Mounted Xsens MTi.

conducted to illustrate this fact with the following parameters: the desired trajectories are generated using the desired angular acceleration $\dot{\omega}_d = [0.4 \sin(0.4t), 0.5 \sin(0.5t + 0.1), 0.3 \sin(t - 0.2)]^T$ (rad/s²). The chosen gains are: $\alpha_1 = \alpha_2 = 1$, $\delta_1 = \delta_2 = 1$, $\rho_1 = \rho_2 = 8$, and $k = 5$. The initial attitude in the Euler angles was taken $(\varphi(0), \theta(0), \psi(0)) = (-30, 15, 5)^\circ$ and $(\varphi_d(0), \theta_d(0), \psi_d(0)) = (0, 0, 0)^\circ$ for rigid body and desired attitude, respectively. All other parameters are taken the same as in Section V-A, except the fact that $\omega_m(t) = \omega(t)$ (without bias). Despite the fact that the chosen noise represents nearly 10% of the amplitude of the measured vectors, the proposed attitude controller tracks the desired attitude successfully, as shown in Fig. 4, where Fig. 4(a)–(c) shows the real quaternion trajectories, the desired quaternion trajectories, and the quaternion errors, respectively. In Fig. 4(d)–(f), the torque τ compared with the raw torque τ_n illustrates the importance of using the filtered measurements.

C. Experimental Tests

Experiments were done based on DIY drone project [21]. We have used the platform shown in Fig. 5(a). It is a test-bench with DIY Quad equipped with the APM2.6 [24] autopilot used for indoor tests. The autopilot APM2.6 is based on Atmel ATMEGA2560-16AU using an external clock of 16 MHz. The embedded system is equipped with Invensense's 6 DoF Accelerometer/Gyro MPU-6000 and a three-axis external compass HMC5883L-TR. The main loop operating frequency of the firmware is 100 Hz. The acquisition of accelerometer and

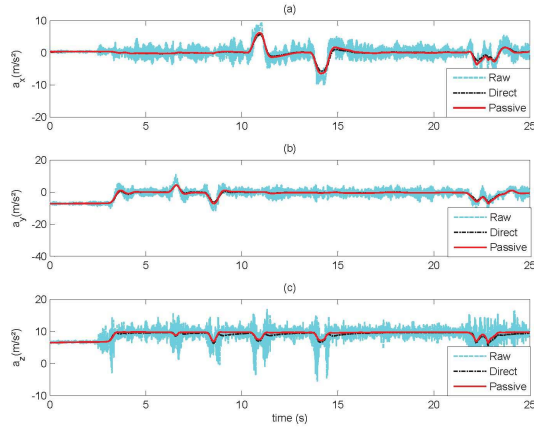


Fig. 6. Raw and filtered accelerometer measurements: (a) For x-axis. (b) For y-axis. (c) For z-axis.

gyros measurements is similar to the main loop, while the frequency acquisition of magnetometer measurements is 10 Hz (after an internal filtering). To validate our results, two main experiments were done. The first one was made to evaluate the performance of our attitude observer using the well-known Xsens MTi AHRS, as shown in Fig. 5(b). In this experiment, the attitude measurements provided by the MTi is considered as a reference signal. The second experiment consists of the implementation of our attitude controller directly on the autopilot APM2.6.

1) *Experimental Test for Attitude Estimation*: As described above, the attitude measurements delivered by the Xsens MTi will be considered as a reference signal for the comparison of results. This reference is obtained with an internal Kalman filter implemented inside MTi. The explicit observer presented in [7] with quaternion formulation was implemented and will be termed MahonyHamelPflimlin (MHP) observer.

Remark 4: To preserve the acquisition frequency of accelerometer and gyros measurements and due to autopilot limitation, only the first-order direct and passive filters given by (23) and (30) were implemented using the first-order Euler integration.

For implementation, the following gains were chosen: $\gamma_{11} = \gamma_{21} = 1$ and $\Gamma_1 = \Gamma_2 = 0.003I_d$ for both two filters, while for MHP observer, the gains presented in [7] were used: $k_P = 1$ and $k_I = 0.3$. The measured initial attitude condition given by MTi was $Q(0) = [0.998, -0.031, -0.029, -0.046]^T$, which was used as an initial condition. For reporting results, we first consider the performance of the data fusion obtained by implemented complementary filters. Then, Fig. 6 shows the experimental results for the direct and passive filters. One can observe that the two complementary filters have good performance, which corroborates the fact that asymptotic stability was demonstrated for both filters. Table II shows the standard deviation of Euler angles obtained by tracking attitude measurements delivered by the Xsens MTi as a reference signal. As explained before, the passive filter is less sensitive to noise, as it is shown in Table II. The comparison presented in Table II illustrates the effectiveness of the proposed solution. The

TABLE II
STANDARD DEVIATION OF EULER ANGLES ERRORS

| | $\sigma_\phi(^{\circ})$ | $\sigma_\theta(^{\circ})$ | $\sigma_\psi(^{\circ})$ |
|-------------------|-------------------------|---------------------------|-------------------------|
| Direct 1st order | 2.5271 | 2.4156 | 5.0922 |
| Passive 1st order | 1.6326 | 1.8181 | 3.2652 |
| MHP | 1.6043 | 2.0757 | 3.5868 |

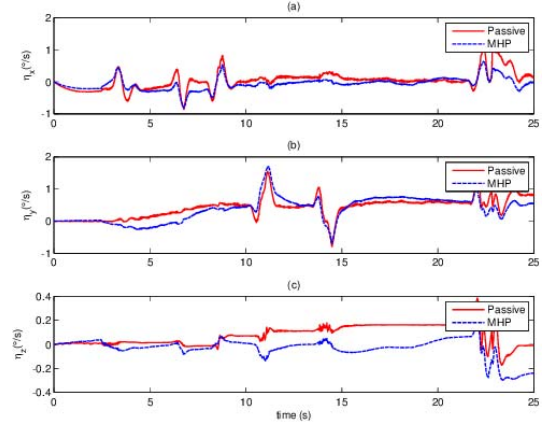


Fig. 7. Rate gyro bias estimation experimental results: (a) For x-axis. (b) For y-axis. (c) For z-axis.

first-order passive filter and the MHP observer give roughly similar results. In Fig. 7, the gyros-bias estimation from both observers is shown.

2) *Attitude Stabilization*: For this test, we considered for simplicity and without loss of generality the special case of stabilization of attitude. The experiment was done using the test-bench shown in Fig. 5(a). The controller (41) was implemented using the following notations and parameters: $R_d(t) = I_d$, which means $b_1^d = r_1$ and $b_2^d = r_2$; $\hat{b}_1 = \hat{a}$ (normalized) and $\hat{b}_2 = \hat{m}$ (normalized) are the estimates of the inertial vector measurements given by the accelerometer and magnetometer, respectively; $\omega_m(t)$ (rad/s) is the rate-gyro measurements considered to be the same as the real one $\omega(t)$; $\rho_1 = 1.66$ and $\rho_2 = 0.1161$ (for the axis x and y), and $\rho_{1z} = 0.05$ and $\rho_{2z} = 0.03$ (for the z -axis); the damping gain $k = 0.2621$ and the filter gains $\alpha_1 = 6$ and $\alpha_2 = 10$.

The main loop for attitude stabilization is running at 100 Hz. At each sampling time, the measurements of accelerometer and magnetometer are normalized after the execution of the observer (32). Due to the poor quality of magnetometer measurements, the gains corresponding to the z -axis are chosen small. Therefore, the stabilization is done around the x and y axes only. Then, starting from an arbitrary measured initial condition in the Euler angles $(\phi, \theta, \psi) = (-18.478, 41.192, 2.847)^{\circ}$, the evolution of normalized inertial measurement vectors, torque, and Euler angles are shown in Fig. 8. We can see that after transient time, the normalized measurements vectors a and m converge to the desired values $b_1^d = [0, 0, 1]^T$ and $b_2^d = [0.434, -0.04, 0.899]^T$. Consequently, according to the attitude estimate, this corresponds to the roll and pitch angles close to zero, which confirms the stabilization of the platform. We can also observe that the control torque is smooth without noise through the use of the complementary filter.

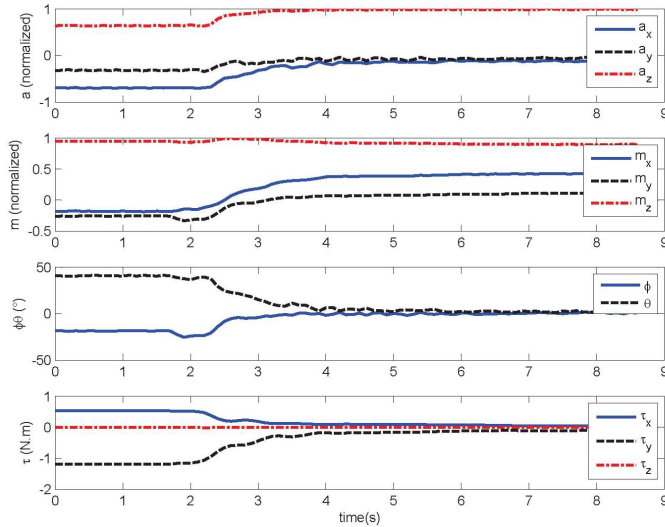


Fig. 8. Attitude stabilization experimental results.

VI. CONCLUSION

Due to its importance and despite the considerable number of solutions, the problem of attitude estimation and control is still relevant. This brief presents high-order direct and passive linearlike complementary filters for attitude and gyro-rate bias estimation. Using the Lyapunov analysis, the proposed solutions ensure global convergence. Another novelty of this brief lies in the proposition of the new control law for sensor-based attitude tracking problem, in which the principle of data fusion is used. Only filtered inertial vectors and rate-gyro measurements were used in the control law, without using attitude measurements and ensuring an almost global stability. To show the efficiency and performance of the proposed solutions, a set of simulation and experimental tests were performed based on DIY drone Quadcopter, equipped with APM2.6 autopilot. The passive second-order filter can be of great help. Indeed, in the future work, this filter will be used to enhance the low sampling frequency of magnetometer measurements compared with that of accelerometer.

APPENDIX PROOF OF LEMMA 1

Showing the thesis amounts to exhibit an example. For that purpose, consider $\gamma = (C_n^l \alpha^l)_{1 \leq l \leq n} \in \mathbb{R}^n$, where n is a positive integer, α is a positive real number, and C_n^l is the binomial coefficient. Then, $P_\gamma(s) = (s + \alpha)^n$ implying that $\gamma \in \mathcal{H}_n$. It remains to show that $\gamma \in \overline{\mathcal{H}}_n$. One clearly has that $P_{\pi(\gamma)} = (P_\gamma(s) - P_\gamma(0))/s$, and thus, the roots of $P_{\pi(\gamma)}$ are the nonzero roots of $(s + \alpha)^n - \alpha^n$. Every root z of the previous polynomial verifies that $((z/\alpha) + 1)^n = 1$, and then, $(z/\alpha) + 1 = e^{j(2k\pi/n)}$, where $j^2 = -1$ and $k = 0, \dots, n-1$. It yields that $\text{Re}(z) = \alpha(\cos(2k\pi/n) - 1)$, which is negative only if $k \neq 0$ and in the latter case $z = 0$. One deduces that all the roots of $P_{\pi(\gamma)}$ have negative real part, i.e., $P_{\pi(\gamma)}$ is Hurwitz, and thus, $\gamma \in \overline{\mathcal{H}}_n$.

REFERENCES

- [1] M. Zamani, J. Trumpf, and R. Mahony. (Feb. 2015). "Nonlinear attitude filtering: A comparison study." [Online]. Available: <http://arxiv.org/abs/1502.03990>.
- [2] N. A. Chaturvedi, A. K. Sanyal, and N. H. McClamroch, "Rigid-body attitude control," *IEEE Control Syst. Mag.*, vol. 31, no. 3, pp. 30–51, Jun. 2011.
- [3] J. L. Crassidis, F. L. Markley, and Y. Cheng, "Survey of nonlinear attitude estimation methods," *J. Guid., Control, Dyn.*, vol. 30, no. 1, pp. 12–28, Jan. 2007.
- [4] M. D. Shuster, "A survey of attitude representations," *J. Astron. Sci.*, vol. 41, no. 4, pp. 439–517, Oct./Dec. 1993.
- [5] M. Euston, P. Coote, R. Mahony, J. Kim, and T. Hamel, "A complementary filter for attitude estimation of a fixed-wing UAV," in *Proc. IEEE/RISJ Int. Conf. Intell. Robots Syst.*, Nice, France, Sep. 2008, pp. 340–345.
- [6] J. Vasconcelos, C. Silvestre, P. Oliveira, P. Batista, and B. Carneira, "Discrete time-varying attitude complementary filter," in *Proc. Amer. Control Conf.*, St. Louis, MO, USA, Jun. 2009, pp. 4056–4061.
- [7] R. Mahony, T. Hamel, and J.-M. Pfifflin, "Nonlinear complementary filters on the special orthogonal group," *IEEE Trans. Autom. Control*, vol. 53, no. 5, pp. 1203–1218, Jun. 2008.
- [8] A. Tayebi, A. Roberts, and A. Benallegue, "Inertial measurements based dynamic attitude estimation and velocity-free attitude stabilization," in *Proc. Amer. Control Conf.*, San Francisco, CA, USA, Jun./Jul. 2011, pp. 1027–1032.
- [9] P. Batista, C. Silvestre, and P. Oliveira, "Sensor-based globally asymptotically stable filters for attitude estimation: Analysis, design, and performance evaluation," *IEEE Trans. Autom. Control*, vol. 57, no. 8, pp. 2095–2100, Aug. 2012.
- [10] L. Benziene, A. Benallegue, and A. El Hadri, "A globally asymptotic attitude estimation using complementary filtering," in *Proc. IEEE Int. Conf. Robot. Biomimetics*, Guangzhou, China, Dec. 2012, pp. 878–883.
- [11] M. D. Shuster, "The TRIAD algorithm as maximum likelihood estimation," *J. Astron. Sci.*, vol. 54, no. 1, pp. 113–123, Mar. 2006.
- [12] A. Benallegue, A. Mokhtari, and L. Fridman, "High-order sliding-mode observer for a quadrotor UAV," *Int. J. Robust Nonlinear Control*, vol. 18, nos. 4–5, pp. 427–440, 2008.
- [13] A. Tayebi, "Unit quaternion-based output feedback for the attitude tracking problem," *IEEE Trans. Autom. Control*, vol. 53, no. 6, pp. 1516–1520, Jul. 2008.
- [14] T. Lee, "Robust adaptive attitude tracking on SO(3) with an application to a quadrotor UAV," *IEEE Trans. Control Syst. Technol.*, vol. 21, no. 5, pp. 1924–1930, Sep. 2013.
- [15] M.-D. Hua, T. Hamel, P. Morin, and C. Samson, "Introduction to feedback control of underactuated VTOL vehicles: A review of basic control design ideas and principles," *IEEE Control Syst.*, vol. 33, no. 1, pp. 61–75, Feb. 2013.
- [16] J. F. Guerrero-Castellanos, N. Marchand, A. Hably, S. Lesecq, and J. Delamare, "Bounded attitude control of rigid bodies: Real-time experimentation to a quadrotor mini-helicopter," *Control Eng. Pract.*, vol. 19, no. 8, pp. 790–797, Aug. 2011.
- [17] A. Tayebi and S. McGilvray, "Attitude stabilization of a VTOL quadrotor aircraft," *IEEE Trans. Control Syst. Technol.*, vol. 14, no. 3, pp. 562–571, May 2006.
- [18] L. Benziene, A. Benallegue, Y. Chitour, and A. Tayebi, "Velocity-free attitude stabilization with inertial vector measurements," *Int. J. Robust Nonlinear Control*, Aug. 2015. [Online]. Available: <http://dx.doi.org/10.1002/rnc.3407>.
- [19] D. Thakur and M. R. Akella, "Gyro-free rigid-body attitude stabilization using only vector measurements," *AIAA J. Guid., Control, Dyn.*, vol. 38, no. 4, pp. 811–818, 2015.
- [20] A. Tayebi, A. Roberts, and A. Benallegue, "Inertial vector measurements based velocity-free attitude stabilization," *IEEE Trans. Autom. Control*, vol. 58, no. 11, pp. 2893–2898, Nov. 2013.
- [21] 3DR. (Jan. 2015). *Multicopter UAV*. [Online]. Available: <http://copter.ardupilot.com/>.
- [22] F. L. Markley and J. L. Crassidis, *Fundamentals of Spacecraft Attitude Determination and Control*. New York, NY, USA: Springer, 2014.
- [23] R. A. Horn and C. R. Johnson, *Topics in Matrix Analysis*. Cambridge, U.K.: Cambridge Univ. Press, 1991.
- [24] 3DR, Berkeley, CA, USA. (Jan. 2015). [Online]. Available: <http://store.3drobotics.com/>.